



A spectroscopic analysis of macrospicules

E. Scullion^{1,2}, J. G. Doyle¹, and R. Erdélyi²

¹ Armagh Observatory, College Hill, Armagh, BT61 9DG, Northern Ireland

² Solar Physics and Space Plasma Research Centre (SP2RC), Department of Applied Mathematics, University of Sheffield, Sheffield, S3 7RH, England
e-mail: ems@arm.ac.uk

Abstract. We explore the nature of macrospicule structures, both off-limb and on-disk, and their possible relation to explosive events in the mid-solar atmosphere. We use high resolution spectroscopy obtained with the SoHO/SUMER instrument. We present a highly resolved spectroscopic analysis and line parameter study of time series data for such jets. We focus on two interesting off-limb events which rapidly propagate between the mid-transition region N IV 765 Å line formation (140 000 K) and the lower corona Ne VIII 770 Å line formation (630 000 K). In one example, a strong jet-like event is associated with a cool feature not present in the Ne VIII 770 Å line radiance or Doppler velocity maps. Our data reveals fast, repetitive plasma outflows with blue-shift velocities of $\approx 145 \text{ km s}^{-1}$ in the lower solar atmosphere. The data suggests a strong role for smaller jets (spicules), as a precursor to macrospicule formation, which may have a common origin with explosive events.

Key words. Methods: data analysis – Methods: observational – Techniques: imaging spectroscopy – Sun: corona– Sun: UV radiation

1. Introduction

The solar transition region (TR) is a very dynamic and thin layer ($\approx 500\text{--}700 \text{ km}$ thick), approximately 2 000 km above the visible photospheric surface of the Sun (Mariska 1992). Jets are highly abundant in the lower to mid solar atmosphere and may provide the key to understanding the powering mechanisms of the TR. Small-scale transient features are continuously seen in chromospheric and transition region (TR) lines. They are classified according to their line profiles, shifts, radiance enhancement, duration and, for off-limb events, height. Jet-like transients are largely respon-

sible for the role of mass and energy transfer from the solar surface to the upper corona and furthermore they are thought to dominate the fast component of the solar wind. However, a clear understanding on how limb events appear when seen on-disk does not exist in the literature.

Giant spicules, named macro-spicules, are observed to reach heights larger than 15 000 km off-limb, can have lifetimes greater than 40 minutes and have been observed as groups of jets with individual lifetimes of 5 min (Bohlin et al. 1975; Xia et al. 2005). Shibata et al. (1992) proposed that all spicules, including mottles, fibrils and macrospicules, result from the same fundamental process

Send offprint requests to: E. Scullion

at different scales. As a result two models have been proposed to explain macrospicule formation (Yamauchi et al. 2004), i. e. the erupting loop model – whereby an emerging closed bipole erupts through the solar atmosphere and reconnections with the ambient closed magnetic fields, and the spiked jet model – explosive magnetic reconnection low in the solar atmosphere accelerates plasma in an explosive release of magnetic energy along open field lines towards the upper atmosphere. Macrospicules have also been closely linked, with respect to duration, temperature range comparison and spatial variation, to TREE’s (Transition Region Explosive Events), as well as blinkers (Harrison 1997; Marik & Erdélyi 2002) which are also strongly associated with TREE’s and even spicule activity (O’Shea et al. 2005; Madjarska & Doyle 2002).

As with macrospicules, spectral analysis has shown that EUV jets exhibit Gaussian ‘wing’ formation with typical velocities of 230 km s^{-1} in Ne VIII ($\log T_e = 5.8$) and $210\text{--}280 \text{ km s}^{-1}$ in C IV ($\log T_e = 5.0$) (Wilhelm et al. 2002). Furthermore, three small X-Ray and EUV jets observed with TRACE (Transition Region and Coronal Explorer, Handy et al. 1999) $171/195 \text{ \AA}$ revealed apparent velocities in the range of $90\text{--}310 \text{ km s}^{-1}$, with lifetimes of $100\text{--}2000 \text{ sec}$. reaching $1.1\text{--}5.0 \times 10^5 \text{ km}$ in height. This result is comparable to earlier observations with Yohkoh SXT.

The recent launch of Hinode (Kosugi et al. 2007) with three on-board instruments, namely, EIS (Extreme Ultraviolet Imaging Spectrometer, Culhane et al. 2007), SOT (Solar Optical Telescope, Tsuneta et al. 2008), and XRT (X-Ray Telescope, Golub et al. 2007) has provided ubiquitous observations of many jets in polar coronal holes (pCHs) as well as evidence of localized regions with very strong kG magnetic fields. Hinode/XRT records jets at an order of magnitude higher rate than previously thought (Cirtain et al. 2007). Consequently, jets may have a more significant impact on the solar atmosphere than previously accounted for (Savcheva et al. 2007; Chifor et al. 2008; Moreno-Insertis et al.

2008). Spectral line fitting of EIS data can give us information on the hot coronal plasma but what is the effect lower in the atmosphere, e. g. the transition region and lower corona? Furthermore, a clear understanding on how limb events appear when seen on-disk still does not exist in the literature. McIntosh & De Pontieu (2009) and Zaqarashvili & Erdélyi (2009) noted several questions concerning the relationship between chromospheric spicules and the emitting transition region structures observed above the limb. In an attempt to address some of these issues, we analyze spectroscopic data taken with the SoHO/SUMER (Solar Heliospheric Observatory/Solar Ultraviolet Measurements of Emitted Radiation) spectrograph (Wilhelm et al. 1995) in pCH regions.

2. Data

The data analyzed here were acquired with the SUMER spectrograph using slit B ($1'' \times 300''$ field of view; $1''$ at L1 corresponds to 715 km on the Sun’s surface). The slit width ($1''$) is the spatial resolution in the x -direction which is the same as the spatial resolution along the y -direction (north-south). The spectral resolution of the instrument is $40 \text{ m\AA pixel}^{-1}$ and we use two windows of 50 pixels each enabling accurate resolution of the two selected emission lines. We study the variation of the emission line profiles for two lines: N IV 765.15 \AA and Ne VIII 770.42 \AA originating around $140\,000 \text{ K}$ (transition region) and $630\,000 \text{ K}$ (low corona), respectively. Instrumental broadening of the spectral line profiles must be considered in order to correctly interpret the FWHM (Full-Width-Half-Maximum) line parameter. We applied a procedure first outlined by Dammasch et al. (1999), shown by Xia et al. (2005), and applied in Popescu et al. (2005, 2007).

3. Results

As shown in Popescu et al. (2007), searching for jet-like or explosive events is greatly enabled through the use of FWHM mapping. Localized events with non-Gaussian spectral

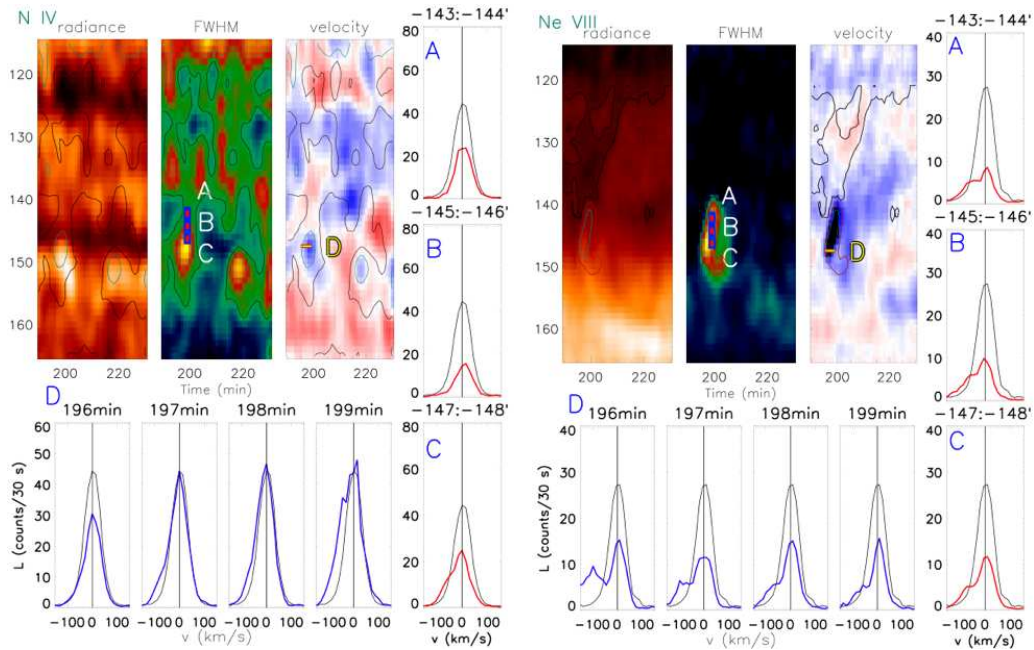


Fig. 1. Time-series radiance, Doppler velocity and width (FWHM) maps in N IV 765 Å (left) and Ne VIII 770 Å (right) for a macrospicule / cool loop event occurring on-disk in the NpCH (Northern polar Coronal Hole). The contours on the radiance and Doppler velocity maps, for the N IV 765 Å line, are the contours of the FWHM data with values of 1.6 spectral pixels (light) and 1.8 spectral pixels (dark). The contour on the radiance and Doppler velocity maps, for the Ne VIII 770 Å line, are the contours of the FWHM data with a value of 2.1 spectral pixels. A contour line of the radiance map is plotted onto the FWHM and Doppler velocity maps.

line profiles appear as bright regions in the FWHM maps. In this section we will focus on a number of these interesting events. We first analyze an on-disk event.

The event shown in Fig. 1 displays a strong FWHM variation at Solar $Y = -149''$, for ≈ 5 – $10''$, over a time interval of ≈ 5 min (between 195 min and 200 min). The temporal variation of the line profiles for this event, as indicated with marker D, show increasing intensity from 196 min until 199 min with some non-Gaussian features growing significantly from $t = 197$ to 199 min. There is a high signal-to-noise ratio given the 30 s exposure time for this observation. The initial jet surge is followed by increased line broadening in the jet. A second event occurs at Solar $Y = -151''$ and at $t = 218$ min with similar activity in the FWHM map, although, with no substantial radiance enhancement. When we inspect the Ne VIII 770 Å

line parameter map for this region (as marked by D profiles), we see a strong Doppler shift in the blue and substantial line broadening along the length of a more extended jet-like structure. From markers A, B and C, we observe that the line profiles exhibit substantial blue wing formation which corresponds to outflow in the range of 80 – 100 km s $^{-1}$. However, when we investigate the line profiles at the source of the jet outflow, we observe even stronger blue shift with a dominant wing formation at $t = 195$ min and $t = 196$ min.

Figure 2 presents the double Gaussian fitting of the locations marked by D in the Ne VIII 770 Å emission. The blue-shifted wing of the emission line is well fitted with a second Gaussian line profile (*dashed*) for the wing component as well as a Gaussian for the line itself (*dotted*). The wing component reaches a maximum of 145 km s $^{-1}$ at $t = 195$ min

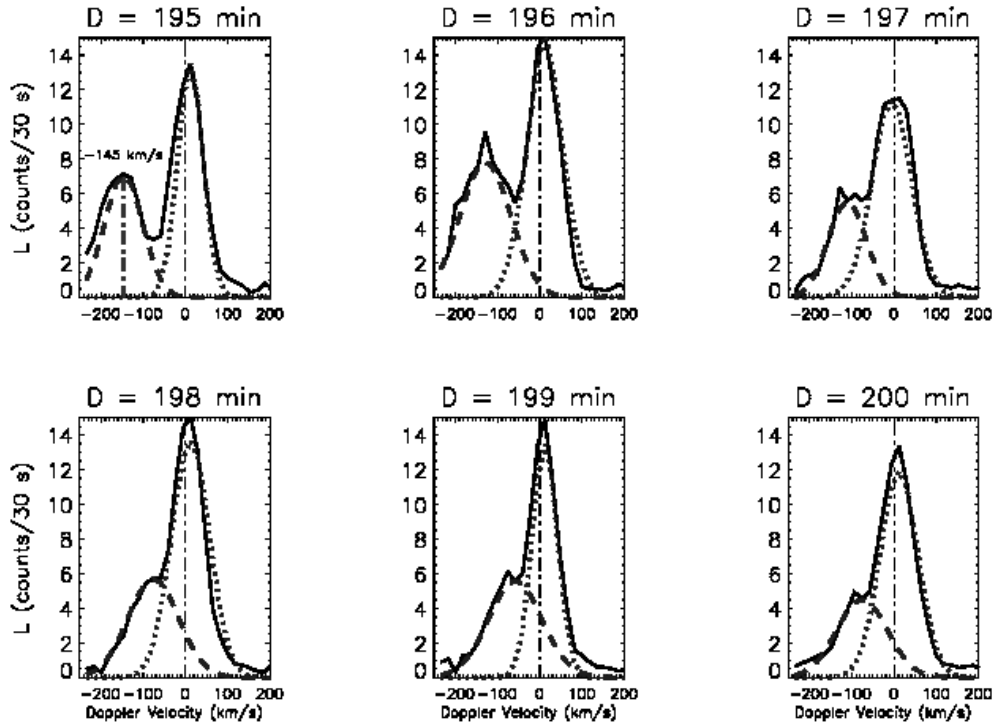


Fig. 2. The Ne VIII 770 Å spectral line profiles for region D have significantly strong wing formation which evolve with time from top left to bottom right. Such spectral line profiles are well fitted with double Gaussian line profiles as demonstrated here. The *solid* lines are the measured spectral line profiles, the *dotted* lines are the fitted Gaussian line profiles for the line centre and the *dashed* lines are the fitted Gaussian line profiles for the wings.

and is shown to evolve over the 5 min interval with decreasing intensity and velocity. Clearly, FWHM mapping is crucial in the identification process of this event in the hotter line. After 5 min, the extent of the line shift declines to 60 km s^{-1} . The stronger signal in Ne VIII 770 Å may indicate that the trigger for this event occurs higher in the solar atmosphere. The activity may then continue downwards to the lower atmosphere creating increased activity in N IV 765 Å within the period from $t = 198 - 200 \text{ min}$.

Next, we turn our attention to an off-limb event. Figure 3 presents an off-limb macrospicule event for the SpCH (Southern polar Coronal Hole) dataset. This event has a distinct three stage morphology which describes a small blue-shifted jet (between $t =$

762 min and $t = 768 \text{ min}$) preceding a dominant red to blue shift in the more extended second jet lasting $\approx 19 \text{ min}$ after the rise of the first jet (between $t = 769 \text{ min}$ and $t = 788 \text{ min}$). Also, the maximum height above the limb of the second stage is $40''$ which is characteristic of macrospicules.

The fast rise of the initially smaller jet from a height of $25''$ at $t = 764 \text{ min}$ to a maximum height of $40''$ in the second stage within 9 min implies a rise velocity of $\sim 20 \text{ km s}^{-1}$. This increased duration in the acceleration stage of the event, including the red-shift region, implies a more energetic jet event. In the line profile variation of marker D, we observe a dominant red-shift of the N IV 765 Å line with a strong wing at $t = 770 \text{ min}$ which can be fitted with a double Gaussian. Its wing component has a

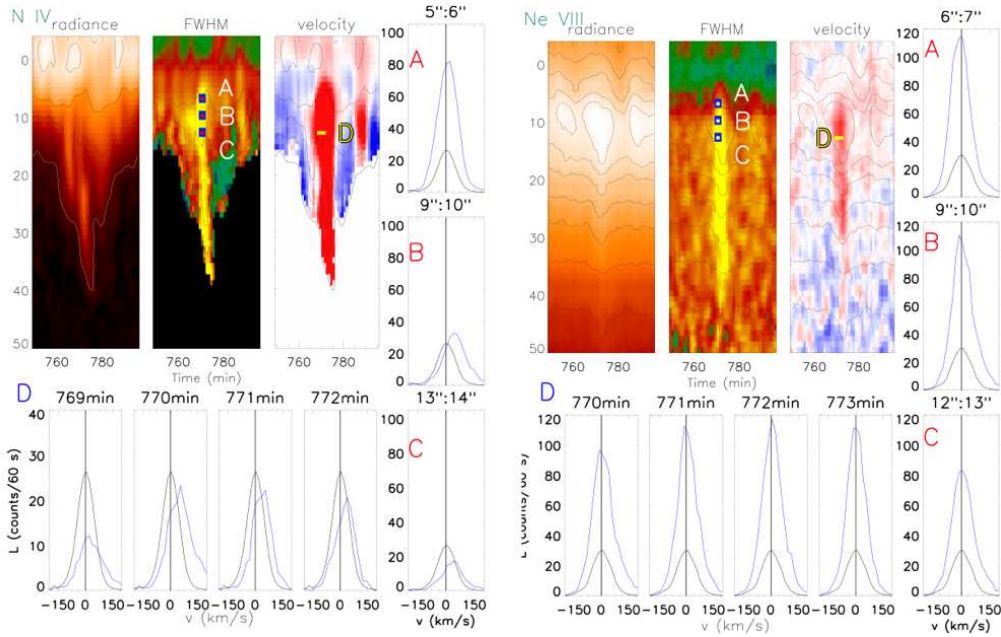


Fig. 3. Time-series radiance, Doppler velocity and width (FWHM) maps in N IV 765 Å (left) and Ne VIII 770 Å (right) for a macrospicule event occurring off-limb in the SPCH. Surrounding each of the line parameter maps are the fitted spectral line profiles representing the locations marked on the maps by A, B, C which describe the spatial evolution of the line at one time. Marker D describes the temporal evolution of the line at one location along the slit. The black line profile represents the mean line profile found through summing all fitted spectral pixel windows on-disk for the full duration of the observation. The contours on the FWHM and Doppler velocity maps, for both lines, are the contours of the radiance data highlighting strong intensity regions in the duration of the event.

velocity of $50\text{--}100\text{ km s}^{-1}$. The extent of this red wing formation declines at $t = 771\text{ min}$ and is no longer present at $t = 772\text{ min}$. Hence, an explosive event occurs between $769\text{--}770\text{ min}$ at $\approx -13''$ accelerating the plasma present in the earlier smaller jet from $\approx 25''$ to $40''$ off-limb with continued red-shift ($10\text{--}15\text{ km s}^{-1}$) until finally evolving into a lesser blue-shifted component.

4. Discussion

The key to understanding the implications of these processes may be found in the observed line width broadening activity in Ne VIII 770 Å. We observed a distinct increase in the Ne VIII 770 Å line width broadening extending from the limb to $40''$ over an interval ($\sim 11\text{ min}$) between $t = 765\text{ min}$ and

$t = 776\text{ min}$ (see Fig. 3). The line profiles for marker D (furthest off-limb) show significant broadening at $\approx 14\text{--}15''$ off-limb with increased radiance compared with the mean spectral line profile (black). At 772 min , the radiance of the line emission is ≈ 6 times greater than the mean line profile. Line broadening is evident in the profiles marked by A, B and C between $6''$ and $13''$ off-limb. This activity in Ne VIII 770 Å is not so obvious in the radiance map (unlike in the radiance map of N IV 765 Å) but this event is strongly observed in the line width map. This observation leads us to believe that some heating may occur in the lower corona. Doyle et al. (2005) suggested that the increase in line broadening off-limb may not be due to small scale random motions but rather a superposition of line shifts due to spicules and/or macrospicule activity.

The three stage morphology of the jet seen off-limb in Fig. 3 may imply a substructure associated with the macrospicule formation. Anomalous resistivity could become important in driving magnetic reconnection as a result of the initial jet propagation (Chen & Priest 2006; Roussev et al. 2001). In other words, an initially smaller wave-driven jet may trigger reconnection between the open and closed magnetic fields and so the smaller jet evolves into a larger jet with a component of the plasma travelling through the cool loop. This description could be applicable to all jets discussed here. The detected on-disk activity in N IV 765 Å, with coinciding activity in Ne VIII 770 Å, is somewhat similar to transition region explosive events (TREEs). These were recently observed to occur in bursts with a period of 3 to 5 min as a result of either kink mode oscillations in closed loops undergoing reconnection (Doyle et al. 2006), or by propagating p -mode oscillations into the upper chromosphere (De Pontieu et al. 2004; De Pontieu & Erdélyi 2006; Chen & Priest 2006). Recent data analyzed by (Doyle et al. 2006) suggest two types of TREEs – one formed in the low chromosphere and the other in the mid-to-high TR.

Recently, McIntosh & De Pontieu (2009) explored a joint observation of the southeast limb with Hinode/SOT Ca II H, TRACE 1600 Å (Transition Region Coronal Explorer) and SUMER (lines Ne VIII 770 Å, N IV 764 Å and O VI 786 Å). A macrospicule was observed and crossed the line-of-sight of the SUMER detector B slit. Space-time analysis with SOT and TRACE revealed jet-ejected material which followed a parabolic trajectory (characteristic of Type I spicules) with velocity of $\sim 40 \text{ km s}^{-1}$ measured after 7 min. This jet was described as being similar to a Type I spicule event though with larger spatial coverage. As discussed, we draw similar conclusions for Fig. 3, although we reveal new heating implications with regards to macrospicules with a longer lasting red-shift phase. Baker et al. (2008) analyzed EIS and XRT observations of on-disk hot jets in coronal holes in multiple wavelengths. They observed a jet with a post-jet increase in its EUV lightcurve. They suggested that this feature arises because the hot

plasma, having failed to reach escape speeds, cools and falls back. They concluded that the fall-back of plasma provided some evidence of impact heating. We need to address more specifically how the ejected material from a macrospicule can become a constituent of the corona and under what circumstances will it become completely ejected and/or fall back. Further statistical analysis of both on-disk and off-limb examples of macrospicule jets in pCH, via a spectroscopic approach, is required.

5. Conclusions

In this paper, we report on finding high velocity features observed simultaneously in spectral lines formed in the mid-transition region (N IV 765 Å) and in the low corona (Ne VIII 770 Å) for both on-disk and off-limb transient and explosive events. The most interesting outcome of this study is the presence of non-Gaussian line profiles showing line of sight up-flows of $\approx 80 \text{ km s}^{-1}$ not only in the cold N IV 765 Å line on disk in Fig. 1, but, also, in the hot Ne VIII 770 Å line where the reported flow speeds become even higher ($\approx 145 \text{ km s}^{-1}$) (as in Fig. 2).

We have shown that spicules can become identifiable on-disk, spectroscopically, as localized plasma outflows in not just the lower solar atmosphere but, also, in the mid-transition region. The events which we have outlined reveal that spicule activity could act as a precursor to macrospicule formation.

Finally, this study highlights the fact that we can advance our understanding of the small-scale structures in the solar atmosphere in the context of how they contribute to two of the big unanswered questions in solar physics: coronal heating and the solar wind's origin and acceleration. To do so we need a high resolution EUV spectrograph (ideally combining a narrow-band EUV imaging telescope plus optical data including magnetograms) that should have improved temporal and spectral resolution in the lower corona and transition region emission lines. More details regarding these results and further analysis of the datasets discussed in this article are outlined in Scullion et al. (2009).

Acknowledgements. Research at Armagh Observatory is grant-aided by the N. Ireland Dept. of Culture, Arts & Leisure. This work was also supported by STFC and the Solar Physics and Space Plasma Research Centre (SP2RC) in the Department of Applied Mathematics at the University of Sheffield, UK. SUMER is financed by DLR, CNES, NASA and ESA PRODEX (Swiss contribution). We thank the EIT team for full-Sun images. SUMER and EIT are part of SoHO, the Solar & Heliospheric Observatory of ESA & NASA. ES would like to acknowledge F Scullion for her thorough grammatical revision of the text. RE acknowledges M. K  ray for patient encouragement. RE is grateful to NSF, Hungary (OTKA, Ref. No. K67746) and the Science and Technology Facilities Council (STFC), UK for the financial support received.

References

- Baker, D., van Driel-Gesztelyi, L., Kamio, S., et al. 2008, in *First Results From Hinode*, ed. S. A. Matthews, J. M. Davis, & L. K. Harra, PASPC, 397, 23
- Bohlin, J. D., Vogel, S. N., Purcell, J. D., et al. 1975, *ApJ*, 197, L133
- Chen, P. F. & Priest, E. R. 2006, *Sol. Phys.*, 238, 313
- Chifor, C., Isobe, H., Mason, H. E., et al. 2008, *A&A*, 491, 279
- Cirtain, J. W., Lundquist, L. L., DeLuca, E. E., et al. 2007, *BAAS*, 38, 222
- Culhane, J. L., Harra, L. K., James, A. M., et al. 2007, *Sol. Phys.*, 243, 19
- Dammasch, I. E., Wilhelm, K., Curdt, W. & Hassler, D. M. 1999, *A&A*, 346, 285
- De Pontieu, B., Erd  lyi, R. & James, S. P. 2004, *Nature*, 430, 536
- De Pontieu, B. & Erd  lyi, R. 2006, *Phil. Trans. R. Soc. London, Ser. A*, 364, 383
- Doyle, J. G., Giannikakis, J., Xia, L. D. & Madjarska, M. S. 2005, *A&A*, 431, L17
- Doyle, J. G., Popescu, M. D. & Taroyan, Y., 2006, *A&A*, 446, 327
- Golub, L., Deluca, E., Austin, G., et al. 2007, *Sol. Phys.*, 243, 63
- Handy, B. N., Acton, L. W., Kankelborg, C. C., et al. 1999, *Sol. Phys.*, 187, 229
- Harrison, R. A. 1997, *Sol. Phys.*, 175, 467
- Kosugi, T., Matsuzaki, K., Sakao, T., et al. 2007, *Sol. Phys.*, 243, 3
- Mariska, J. T. 1992, in *The Solar Transition Region* (Cambridge University Press, New York)
- Marik, D. & Erd  lyi, R. 2002, *A&A*, 393, L73
- Moreno-Insertis, F., Galsgaard, K. & Ugarte-Urra, I. 2008, *ApJ*, 673, L211
- Madjarska, M. S. & Doyle, J. G. 2002, *A&A*, 382, 319
- McIntosh, S. W. & De Pontieu, B. 2009, in press
- O'Shea, E., Banerjee, D., & Doyle, J. G. 2005, *A&A*, 436, L43
- Popescu, M. D., Banerjee, D., O'Shea, E., Doyle, J. G. & Xia, L. D. 2005, *A&A*, 442, 1087
- Popescu, M.D., Xia, L. D., Banerjee, D. & Doyle, J. G. 2007, *Advances in Space Research*, 40, 1021
- Roussev, I., Galsgaard, K., Erd  lyi, R., Doyle, J. G. 2001, *A&A*, 370, 298
- Savcheva, A., Cirtain, J., Deluca, E. E., et al. 2007, *PASJ*, 59, 771
- Scullion, E., Popescu, M. D., Banerjee, D., Doyle, J. G., & Erd  lyi, R. 2009, *ApJ*, 704, 1385
- Shibata, K., Nozawa, S., & Matsumoto, R. 1992, *PASJ*, 44, 265
- Tsuneta, S., Ichimoto, K., Katsukawa, Y., et al. 2008, *Sol. Phys.*, 249, 167
- Wilhelm, K., Curdt, W., Marsch, E., et al. 1995, *Sol. Phys.*, 162, 189
- Wilhelm, K., Dammasch, I. E. & Hassler, D. M. 2002, *Ap&SS*, 282, 189-207
- Xia, L. D. 2003, PhD Thesis, Georg-August-Univ., G  ttingen
- Xia, L.D., Popescu, M. D., Doyle, J. G., & Giannikakis, J. 2005, *A&A*, 438, 1115
- Yamauchi, Y., Moore, R. L., Suess, S. T., Wang, H., & Sakurai, T. 2004, in *The Solar-B Mission and the Forefront of Solar Physics*, ed. T. Sakurai & T. Sekii, PASPC, 325, 301
- Zaqarashvili, T. V., Erd  lyi, R. 2009, ArXiv e-prints, eprint 0906.1783